Journal of Molecular Liquids 211 (2015) 256–267

Contents lists available at ScienceDirect

Journal of Molecular Liquids

journal homepage: www.elsevier.com/locate/molliq

Molecular docking, theoretical calculations and potentiometric studies of some azo phenols

A.A. El-Bindary [a,*], M.A. Hussein [b], R.A. El-Boz [a,1]

[a] Chemistry Department, Faculty of Science, University of Damietta, Damietta 34517, Egypt
[b] Chemistry Department, Faculty of Science, University of Port Said, Egypt

ARTICLE INFO

Article history:
Received 6 June 2015
Received in revised form 27 June 2015
Accepted 30 June 2015
Available online xxxx

Keywords:
Azo phenols
Theoretical calculations
Molecular docking
Potentiometry

ABSTRACT

The ligands 5-amino-2-(phenyldiazenyl)phenol and its derivatives ($\mathbf{HL_n}$) were synthesized from the coupling of 3-aminophenol with aniline and its *p*-derivatives and characterized by different spectroscopic techniques. The molecular and electronic structures of the investigated compounds ($\mathbf{HL_n}$) were also studied using quantum chemical calculations. Molecular docking was used to predict the binding between azo compounds with the receptor of prostate cancer 2q7k-Hormone and 3hb5-oxidoreductase receptor of breast cancer. The proton–ligand dissociation constant of the azo compounds ($\mathbf{HL_n}$) and metal–ligand stability constants of their complexes with metal ions (Mn^{2+}, Co^{2+}, Ni^{2+} and Cu^{2+}) have been determined by potentiometric technique in 0.1 M KCl and 40% (by volume) DMF–water mixture. For the same ligand at constant temperature, the stability constants of the formed complexes increase in the order Mn^{2+}, Co^{2+}, Ni^{2+} and Cu^{2+}. The effect of temperature was studied at 303, 313 and 323 K and the corresponding thermodynamic parameters (ΔG, ΔH and ΔS) were derived and discussed. The dissociation process is non-spontaneous, endothermic and entropic ally unfavorable. The formation of the metal complexes has been found to be spontaneous, endothermic and entropic ally favorable.

1. Introduction

Aminophenols have aroused interest owing to their utility as starting materials for many azodyes [1], corrosion inhibitors [2], bactericides [3] and anti-inflammatory agent [4]. From the complexing point of view, many have taken interest in studying aminophenol as potential ligands [5]. Azo colorings are the most versatile class of dyes [6]. The dyes have been most widely used in fields such as dying textile fibers, biomedical studies, advanced applications in organic synthesis and high technology areas like lasers, liquid crystalline displays, electro-optical devices and ink-jet printer [7]. The presence of —N═N— group can lead to increase the solubility of low valent metal oxidation states due to its π acidity and presence of low lying azo centered π* molecular orbitals [8].

Potentiometry is one of the most convenient and successful techniques employed for metal complex equilibrium measurements. In recent years the use of protein–ligand docking has become a standard method in potentiometric studies. The protein groups surrounding the ligand can highly influence the local pH, so that a different protonation could be favored in the bound state. To account for this effect, the ideal case would be to use multiple protonations in the docking and have the algorithm automatically pick the correct state. Molecular docking is widely used to predict protein–ligand [9,10] and to screen large libraries for molecules that will modulate the activity of a biological receptor. In continuation of our previous work [11–15], we report herein the dissociation constant of ($\mathbf{HL_n}$) and the stability constants of their complexes with Mn^{2+}, Co^{2+}, Ni^{2+} and Cu^{2+} at different temperatures. The corresponding thermodynamic functions are evaluated and discussed. Moreover, the molecular and electronic structures of the investigated compounds ($\mathbf{HL_n}$) are also studied using quantum chemical calculations. Molecular docking was used to predict the binding between azo compounds and the receptors of prostate cancer and breast cancer.

2. Materials and methods

2.1. Measurements

All the compounds and solvents used were purchased from Aldrich and Sigma and used as received without further purification. Elemental microanalyses of the separated ligands for C, H, and N were determined on Automatic Analyzer CHNS Vario ELIII, Germany. FT-IR spectra (KBr discs, 4000–400 cm^{-1}) by Jasco-4100 spectrophotometer. The calculations of geometry optimization were performed using Perkin Elmer ChemBio 3D software by HF method with 3-21G basis set [16,17]. Geometry optimization option was employed to obtain the most stable structure. The pH measurements were performed with a Metrohm 836 Titrando (KF & Potentiometric Titrator) equipped with a combined porolyte electrode. The pH-meter readings in the non-aqueous medium

* Corresponding author.
E-mail address: abindary@yahoo.com (A.A. El-Bindary).
[1] Abstracted from her Ph.D. Thesis.

http://dx.doi.org/10.1016/j.molliq.2015.06.070
0167-7322/

were corrected [18]. The electrode system was calibrated according to the method of Irving et al. [19]. The temperature was controlled to within ±0.05 K by circulating thermostated water (Neslab 2 RTE 220) through the outer jacket of the vessel.

2.2. Preparation of the ligands

The ligands 5-amino-2-(phenyldiazenyl)phenol and its derivatives (**HL_n**) were prepared by dissolving aniline or its *p*-substituted derivatives (10 mmol) in conc. H_2SO_4. The compound was diazotized below −5 °C in an ice–salt bath with a solution of sodium nitrite (0.8 g, 10 mmol, 30 ml distilled H_2O). The diazonium salt was coupled with an alkaline solution of 3-aminophenol (1.0 g, 10 mmol) in 20 ml of ethanol. The precipitate was filtered and dried after through washing with water and ethanol. The crude product was recrystallized from ethanol and the microcrystals were obtained in a yield of 94–97% (Fig. 1). The resulting formed ligands are 5-amino-2-((4-methylphenyl)diazenyl)phenol (**HL_1**), 5-amino-2-(phenyldiazenyl)phenol (**HL_2**) and 5-amino-2-((4-chlorophenyl)diazenyl)phenol (**HL_3**).

2.3. Potentiometric studies

A ligand solution (0.01 M) was prepared by dissolving an accurately weighted amount of the solid in DMF. Metal ion solutions (0.001 M) were prepared from metal chlorides in bidistilled water and standardized with EDTA [20]. Solutions of 0.01 M HCl and 1 M KCl were also prepared in bidistilled water. A carbonate-free NaOH solution in 40% (by volume) DMF–water mixture was used as titrant and standardized against oxalic acid.

The apparatus, general conditions and methods of calculation were the same as in previous work [11–15]. The following mixtures (i)–(iii) were prepared and titrated potentiometrically at 298 K against standard 0.02 M NaOH in a 40% (by volume) DMF–water mixture:

i) 5 cm^3 0.01 M HCl + 5 cm^3 1 M KCl + 20 cm^3 DMF.
ii) 5 cm^3 0.01 M HCl + 5 cm^3 1 M KCl + 15 cm^3 DMF + 5 cm^3 0.01 M ligand.
iii) 5 cm^3 0.01 M HCl + 5 cm^3 1 M KCl + 15 cm^3 DMF + 5 cm^3 0.01 M ligand + 10 cm^3 0.001 M metal chloride.

For each mixture, the volume was made up to 50 cm^3 with bidistilled water before the titration. These titrations were repeated for the temperatures of 308 and 318 K. All titrations have been carried out between pH 4.0–11.0 and under nitrogen atmosphere.

3. Results and discussion

3.1. Characterization of the ligands (HL_n)

The chemical structures of the ligands were elucidated by elemental analyses Table 1. The infrared spectra of ligands shows a broad band located at the region 2946–3158 cm^{-1} due to ν(OH) group. The two bands appear at the region 3320–3359 cm^{-1} are due to ν(NH_2). The ν(N═N) group appeared at 1481–1623 cm^{-1} region. The bands at 2603–2711 cm^{-1} region are assigned to ν(C–H) vibrations of the aromatic system.

3.2. Molecular structure

The optimized structures, bond length and bond angles of the (HL_n) ligands are presented in Fig. 2 and Tables 2 and 3. Both the highest occupied molecular orbital (HOMO) and lowest unoccupied molecular orbital (LUMO) are the main orbital which take part in chemical stability. The HOMO represents the ability to donate an electron; LUMO as an electron acceptor represents the ability to obtain an electron as shown in Fig. 3. Quantum chemical parameters of the ligands (HL_n) are obtained from calculations such as energies of the highest occupied molecular orbital (E_{HOMO}) and the lowest unoccupied molecular orbital (E_{LUMO}) as listed in Table 4. Additional parameters such as HOMO–LUMO energy gap, ΔE, absolute electronegativities, χ, chemical potentials, Pi, absolute hardness, η, absolute softness, σ, global electrophilicity, ω, global softness, *S*, and additional electronic charge, ΔN_{max}, are calculated using the following equations [15,21–23]:

$$\Delta E = E_{LUMO} - E_{HOMO} \quad (1)$$

$$\chi = \frac{-(E_{HOMO} + E_{LUMO})}{2} \quad (2)$$

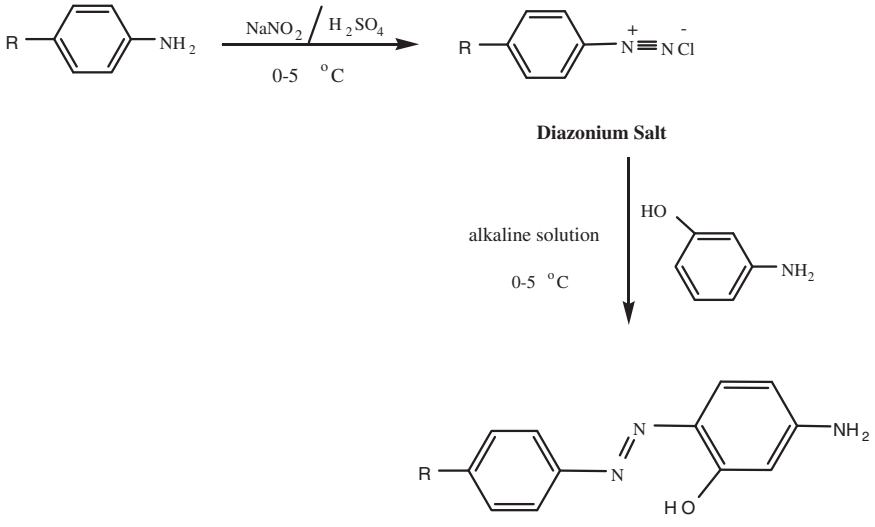

R = -CH_3 (**HL_1**), -H (**HL_2**) and -Cl (**HL_3**).

Fig. 1. Structure of the azo phenols (**HL_n**).

Table 1
Analytical data of the azo phenols (HL_n).

Compound	Empirical formula	Yield %	M.P. °C	Exp. (calc.) %		
				C	H	N
HL_1	$C_{13}H_{13}N_3O$ Orange	94	172	68.72 (68.82)	5.16 (5.33)	19.72 (19.35)
HL_2	$C_{12}H_{11}N_3O$ Dark orange	97	215	67.60 (67.67)	5.16 (5.26)	19.72 (19.42)
HL_3	$C_{12}H_{10}N_3OCl$ Pale orange	96	211	58.18 (58.32)	4.04 (4.24)	16.96 (17.27)

$$\eta = \frac{E_{LUMO} - E_{HOMO}}{2} \quad (3)$$

$$\sigma = \frac{1}{\eta} \quad (4)$$

$$Pi = -\chi \quad (5)$$

$$S = \frac{1}{2\eta} \quad (6)$$

$$\omega = \frac{Pi^2}{2\eta} \quad (7)$$

$$\Delta N_{max} = -\frac{Pi}{\eta}. \quad (8)$$

3.3. Molecular docking

Cancer can be described as the uncontrolled growth of abnormal cells. Prostate cancer is the most common non-skin malignancy in men. Except for lung cancer, it is responsible for more deaths than any other cancer. The American Cancer Society (ACS) estimated 1 man in 6 will be diagnosed with prostate cancer during his lifetime. A little over 1.8 million men in the United States are survivors of prostate cancer [24].

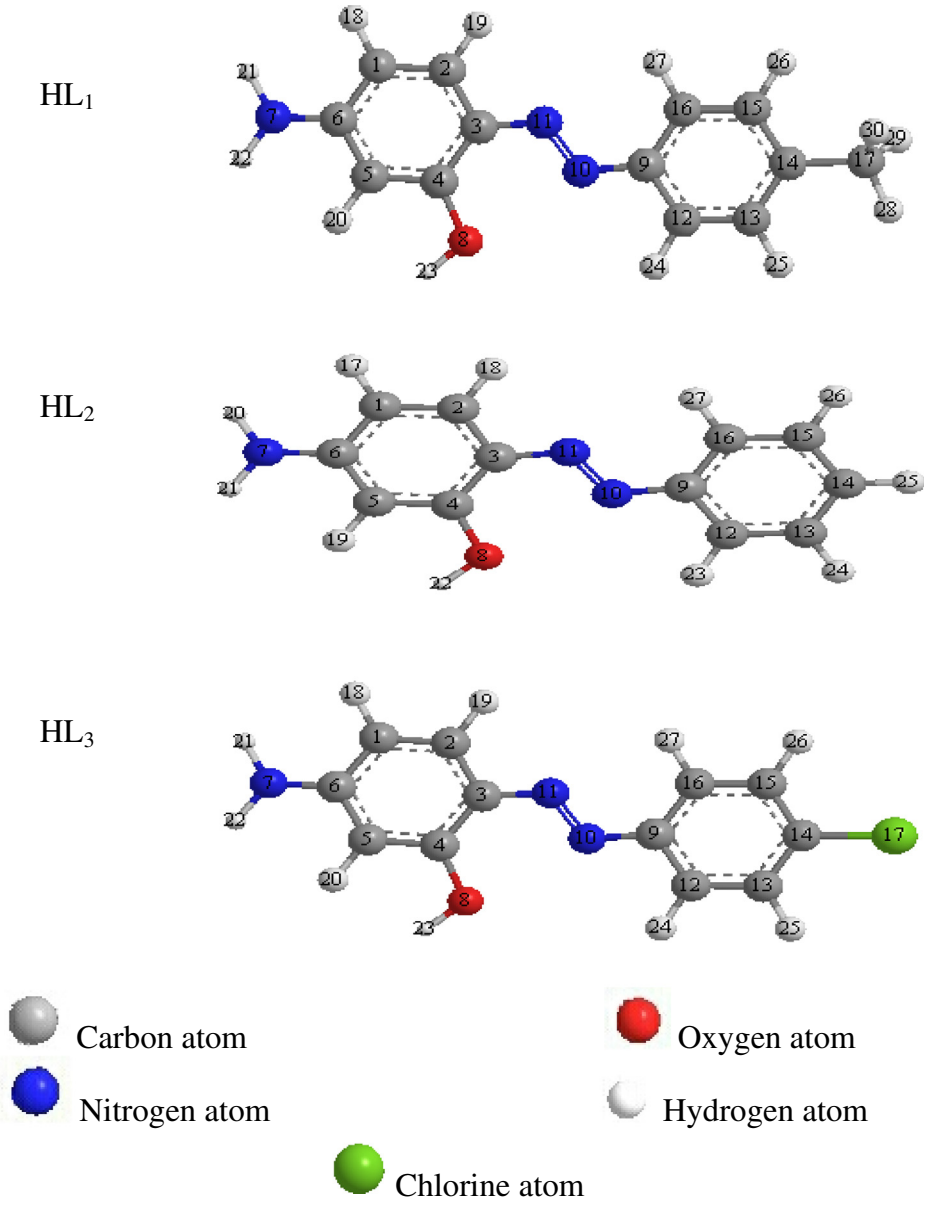

Fig. 2. The calculated molecular structures of the azo phenols (HL_n).

Table 2
The bond length for (HL_n).

Bond length (Å)					
HL_1		HL_2		HL_3	
C(17)–H(30)	1.114	N(15)–N(16)	1.248	N(15)–N(16)	1.251
C(17)–H(29)	1.114	O(14)–H(27)	0.972	O(14)–H(27)	0.971
C(17)–H(28)	1.113	N(13)–H(26)	1.050	N(13)–H(26)	1.049
O(14)–H(27)	0.971	N(13)–H(25)	1.050	N(13)–H(25)	1.049
N(13)–H(26)	1.049	C(12)–H(24)	1.100	C(12)–H(24)	1.103
N(13)–H(25)	1.049	C(11)–H(23)	1.100	C(11)–H(23)	1.103
C(12)–H(24)	1.103	C(11)–C(12)	1.420	C(11)–C(12)	1.343
C(11)–H(23)	1.103	C(10)–H(22)	1.100	C(10)–Cl(17)	1.727
C(9)–H(22)	1.103	C(10)–C(11)	1.420	C(10)–C(11)	1.342
C(8)–H(21)	1.105	C(9)–H(21)	1.100	C(9)–H(22)	1.103
C(6)–H(20)	1.104	C(9)–C(10)	1.420	C(9)–C(10)	1.341
C(3)–H(19)	1.105	C(8)–H(20)	1.100	C(8)–H(21)	1.105
C(2)–H(18)	1.103	C(8)–C(9)	1.420	C(8)–C(9)	1.342
N(15)–N(16)	1.251	N(16)–C(7)	1.456	C(7)–N(16)	1.269
C(11)–C(12)	1.343	C(7)–C(12)	1.420	C(7)–C(12)	1.348
C(10)–C(17)	1.510	C(7)–C(8)	1.420	C(7)–C(8)	1.348
C(10)–C(11)	1.344	C(6)–H(19)	1.100	C(6)–H(20)	1.104
C(9)–C(10)	1.343	C(5)–O(14)	1.355	C(5)–O(14)	1.363
C(8)–C(9)	1.342	C(5)–C(6)	1.420	C(5)–C(6)	1.347
C(7)–N(16)	1.269	C(4)–N(15)	1.456	C(4)–N(15)	1.270
C(7)–C(12)	1.347	C(4)–C(5)	1.420	C(4)–C(5)	1.354
C(7)–C(8)	1.347	C(3)–H(18)	1.100	C(3)–H(19)	1.105
C(5)–O(14)	1.363	C(3)–C(4)	1.420	C(3)–C(4)	1.349
C(5)–C(6)	1.347	C(2)–H(17)	1.100	C(2)–H(18)	1.103
C(4)–N(15)	1.270	C(2)–C(3)	1.420	C(2)–C(3)	1.341
C(4)–C(5)	1.354	C(1)–N(13)	1.462	C(1)–N(13)	1.267
C(3)–C(4)	1.349	C(1)–C(6)	1.420	C(1)–C(6)	1.341

Breast cancer is one of the most recurring worldwide diagnosed and deadliest cancers next to lung cancer with a high number of mortality rates among females [25]. At global level, it accounted for more than 1.6 million new cases in 2010. The incidence or prevalence rate of the breast cancer in India is expected to be more than 90,000 in the coming years and over 50,000 women die each year.

Table 3
The selected geometric parameters bond angle for (HL_n).

Bond angles (°)	HL_1	H_2	HL_3
H(26)–C(15)–C(16)	119.435	120.033	119.326
H(26)–C(15)–C(14)	119.296	119.644	120.487
C(16)–C(15)–C(14)	121.27	120.323	120.188
C(15)–C(14)–C(13)	117.919	119.392	119.509
H(25)–C(13)–C(14)	119.983	120.289	120.73
C(14)–C(13)–C(12)	120.824	119.982	119.847
H(27)–C(16)–C(9)	121.85	121.886	121.799
H(27)–C(16)–C(15)	117.101	117.026	117.009
C(9)–C(16)–C(15)	121.049	121.088	121.191
H(24)–C(12)–C(13)	118.209	120.124	118.139
C(13)–C(12)–C(9)	121.53	121.479	121.583
C(16)–C(9)–C(12)	117.408	117.736	117.682
C(16)–C(9)–N(10)	125.954	125.829	125.849
C(12)–C(9)–N(10)	116.637	116.436	116.469
N(11)–N(10)–C(9)	119.84	119.902	119.87
H(21)–N(7)–C(6)	120.107	120.3	120.111
C(1)–C(6)–C(5)	118.987	118.988	118.991
C(1)–C(6)–N(7)	120.399	120.409	120.401
C(5)–C(6)–N(7)	120.614	120.603	120.609
C(6)–C(5)–C(4)	122.406	122.405	122.404
C(3)–N(11)–N(10)	121.157	121.129	121.153
C(5)–C(4)–C(3)	118.569	118.571	118.566
C(5)–C(4)–O(8)	117.646	117.639	117.658
C(3)–C(4)–O(8)	123.785	123.79	123.776
C(4)–C(3)–C(2)	118.657	118.655	118.663
C(4)–C(3)–N(11)	127.28	127.271	127.253
C(2)–C(3)–N(11)	114.063	114.074	114.084
C(3)–C(2)–C(1)	122.092	122.092	122.087
H(18)–C(1)–C(6)	120.833	120.487	120.835
H(18)–C(1)–C(2)	119.878	117.422	119.876
C(6)–C(1)–C(2)	119.289	119.29	119.289
H(23)–O(8)–C(4)	109.265		109.299
H(20)–C(5)–C(6)	119.181		119.187
H(20)–C(5)–C(4)	118.414		118.409

Docking study showed the binding affinity, number of hydrogen bonds. It is interesting to note that the binding affinities have negative values. This reveals the high feasibility of this reaction. Molecular docking is a key tool in computer drug design [26,27]. The focus of molecular docking is to simulate the molecular recognition process. Molecular docking aims to achieve an optimized conformation for both the protein and drug with relative orientation between them such that the free energy of the overall system is minimized.

The study simulates the actual docking process in which the ligand–protein pair-wise interaction energies are calculated using Docking Server [28]. The MMFF94 Force field was used for energy minimization of ligand molecules using Docking Server. Gasteiger partial charges were added to the ligand atoms. Non-polar hydrogen atoms were merged, and rotatable bonds were defined. Docking calculations were carried out on 2q7k and 3hb5-oxidoreductase–Hormone protein model. Essential hydrogen atoms, Kollman united atom type charges, and solvation parameters were added with the aid of AutoDock tools [29]. Affinity (grid) maps of 0.375 Å spacing were generated using the Autogrid program [30]. AutoDock parameter set- and distance-dependent dielectric functions were used in the calculation of the van der Waals and the electrostatic terms, respectively.

Docking simulations were performed using the Lamarckian genetic algorithm (LGA) and the Solis & Wets local search method [31]. Initial position, orientation, and torsions of the ligand molecules were set randomly. All rotatable torsions were released during docking. Each docking experiment was derived from 10 different runs that were set to terminate after a maximum of 250,000 energy evaluations. The population size was set to 150. During the search, a translational step of 0.2 Å, and quaternion and torsion steps of 5 were applied.

In this context, the docked ligands were analysis with the prostate cancer mutant 2q7k-Hormone and breast cancer 3hb5 as shown in Fig. 4(A, C, E) and (B, D, F) and Fig. 5(A_1, C_1, E_1) and (B_1, D_1, F_1). The study simulates the actual docking process in which the ligand–protein pair-wise interaction energies are calculated in Tables 5 and 6. According to our results, HB plot curve indicates that, azo compound binds to the two proteins with hydrogen bond interactions of ligands (HL_n) with 2q7k and 3hb5 as shown in Figs. 6 and 7. The calculated efficiency is favorable, Ki values estimated by AutoDock were compared with experimental Ki values, when available, and the Gibbs free energy is negative. Also, based on this data, we can propose that interaction between the 2q7k, 3hb5 receptors and the ligands (HL_n) is possible. 2D plot curve of docking with ligands (HL_n) is shown in Figs. 8 and 9. This interaction could activate apoptosis in cancer cell energy of interactions with ligands (HL_n). From the analysis of the values, it is evident that the binding energy of (HL_n) decreases. So that is decrease in binding energy of HLn on transpiration of mutation for prostate cancer 2q7k whereas increase with HLn for breast cancer. Binding energies are most widely used mode of measuring binding affinity of a ligand. Thus, the decrease in binding energy due to mutation will increase the binding affinity of the azo phenol towards the receptor. The characteristic feature of azo phenols represents the presence of several active sites available for hydrogen bonding. This feature gives them the ability to be good binding inhibitors to the protein and will help to produce augmented inhibitory compounds. The results confirm that, the azo ligand derived from 3-aminophenol is an efficient inhibitor of prostate cancer mutant 2q7k-Hormone and 3hb5-oxidoreductase breast cancer.

3.4. Potentiometric studies

The average number of the protons associated with ligands (HL_n) at different pH values, $\overline{n}_A$, was calculated from the titration curves of

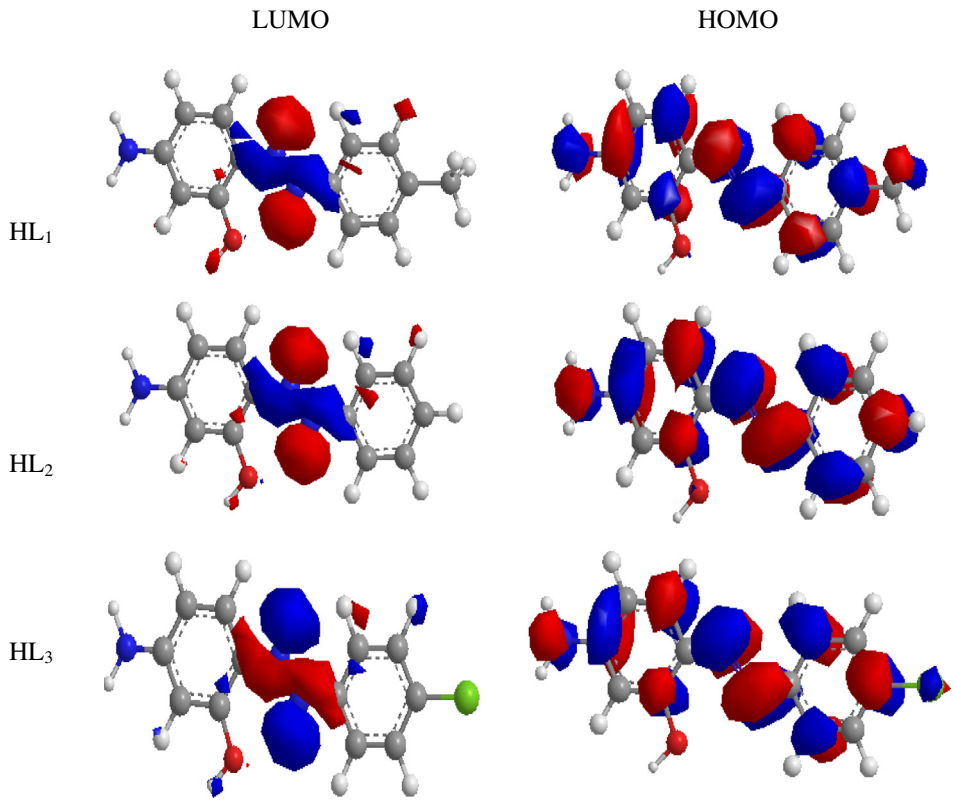

Fig. 3. The highest occupied molecular orbital (HOMO) and the lowest unoccupied molecular orbital (LUMO) of the azo phenols (**HL_n**).

the acid in the absence and presence of ligands (HL_n) by applying the following equation:

$$\bar{n}_A = Y \pm \frac{(V_1 - V_2)(N^\circ + E^\circ)}{(V^\circ - V_1)TC_L^\circ} \quad (9)$$

where Y is the number of available protons in ligands (Y = 1) and V_1 and V_2 are the volumes of alkali required to reach the same pH on the titration curve of hydrochloric acid and reagent, respectively, V° is the initial volume (50 cm^3) of the mixture, TC_L° is the total concentration of the reagent, N° is the normality of sodium hydroxide solution and E° is the initial concentration of the free acid. Thus, the formation curves ($\bar{n}_A$ vs. pH) for the proton–ligand systems were constructed and found to extend between 0 and 1 in the $\bar{n}_A$ scale. This means that azo aminophenol has one ionizable proton (the enolized hydrogen ion of the phenolic –OH group, pK^H). Different computational methods were applied to evaluate the dissociation constant [32]. Three replicate titrations were performed; the average values obtained are listed in Table 7. The completely protonated form of ligands (HL_n) has one dissociable proton, that dissociates in the measurable pH range. The deprotonation of the hydroxyl group most probably results in the formation of stable intramolecular H-bonding with nitrogen of the azo group. Such an interaction decreases the dissociation process of phenolic –OH group, i.e. increases the pK^H value [33,34].

The formation curves for the metal complexes were obtained by plotting the average number of ligands attached per metal ion ($\bar{n}_A$) vs. the free ligand exponent (pL), according to Rossotti and Rossotti [35]. The average number of the reagent molecules attached per metal ion, $\bar{n}$, and free ligand exponent, pL, can be calculated using Eqs. (10) and (11):

$$\bar{n} = \frac{(V_3 - V_2)(N^\circ + E^\circ)}{(V^\circ - V_2)\cdot \bar{n}_A \cdot TC_M^\circ} \quad (10)$$

and

$$pL = \log_{10} \frac{\sum_{n=o}^{n=J} \beta_n^H \left(\frac{1}{[H^+]}\right)^n}{TC_L^\circ - \bar{n}\cdot TC_M^\circ} \cdot \frac{V^\circ + V_3}{V^\circ} \quad (11)$$

where TC_M° is the total concentration of the metal ion present in the solution, β_n^H is the overall proton-reagent stability constant. V_1, V_2 and V_3 are the volumes of alkali required to reach the same pH on the titration curves of hydrochloric acid, organic ligand and complex, respectively. These curves were analyzed and the successive metal–ligand stability constants were determined using different computational methods [36,37]. The values of the stability constants (log K_1

Table 4
The calculated quantum chemical parameters for the azo phenols (**HL_n**).

Compound	E_{HOMO} (eV)	E_{LUMO} (eV)	ΔE (eV)	χ (eV)	η (eV)	σ $(eV)^{-1}$	Pi (eV)	S $(eV)^{-1}$	ω (eV)	ΔN_{max}
HL_1	−3.061	−1.841	1.22	2.451	0.61	1.639	−2.451	0.819	4.924	4.0180
HL_2	−3.218	−1.838	1.38	2.528	0.69	1.449	−2.528	0.725	4.631	3.664
HL_3	−2.733	−1.836	0.89	2.285	0.45	2.229	−2.285	1.115	5.818	5.094

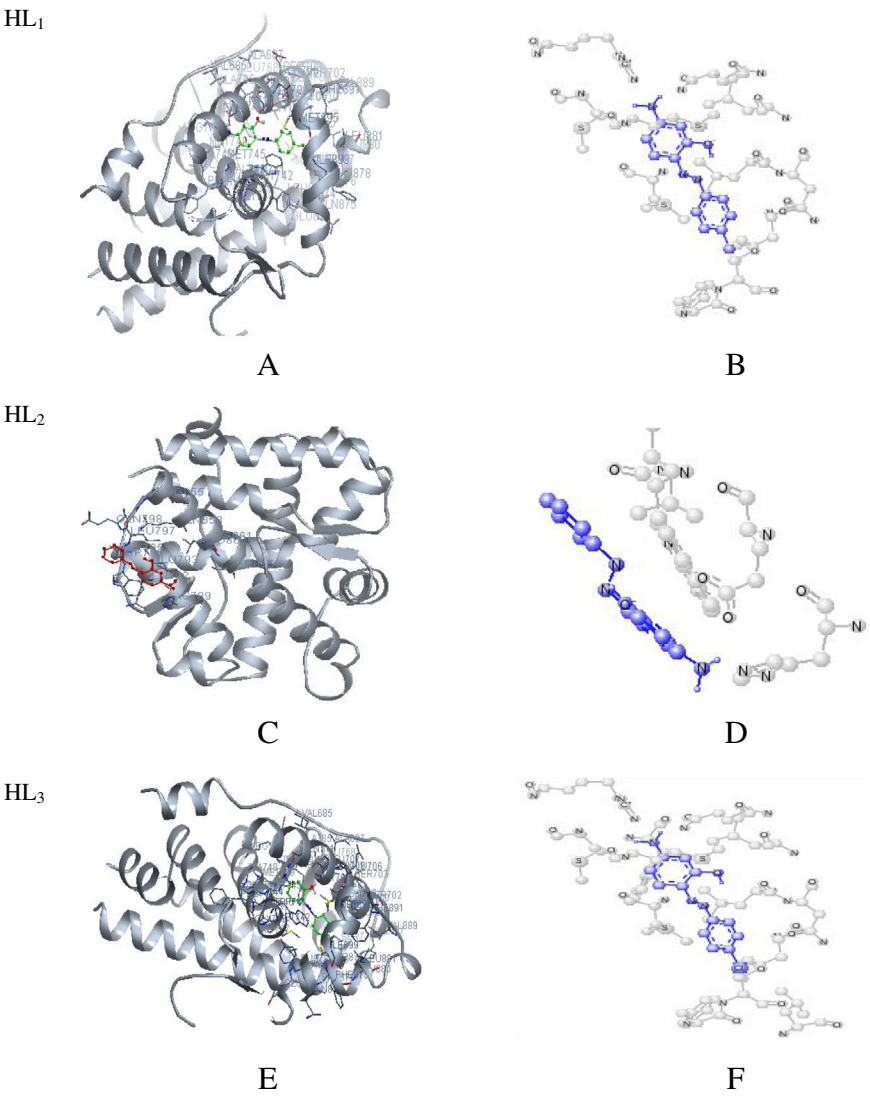

Fig. 4. The azo phenols (**HL_n**) (green in (A, C, E) and blue in (B, D, F)) in interaction with receptor prostate cancer mutant 2q7k. (For interpretation of the references to color in this figure legend, the reader is referred to the web version of this article.)

and log K_2) are given in Table 8. The following general remarks can be pointed out:

(i) The maximum value of $\bar{n}_A$ was ~2 indicating the formation of 1:1 and 1:2 (metal:ligand) complexes only [11,38].
(ii) The metal ion solution used in the present study was very dilute (2×10^{-4} M), hence there was no possibility of formation of polynuclear complexes [39,40].
(iii) The metal titration curves were displaced to the right-hand side of the ligand titration curves along the volume axis, indicating proton release upon complex formation of the metal ion with the ligand. The large decrease in pH for the metal titration curves relative to ligand titration curves points to the formation of strong metal complexes [41,42].
(iv) For the same ligand at constant temperature, the stability of the chelates increases in the order Mn^{2+}, Co^{2+}, Ni^{2+} and Cu^{2+} [43,44]. This order largely reflects that the stability of Cu^{2+} complexes is considerably larger than those of other metals of the 3d series. Under the influence of both the polarizing ability of the metal ion and the ligand field [45] Cu^{2+} will receive some extra stabilization due to tetragonal distortion of octahedral symmetry in its complexes. The greater stability of Cu^{2+} complexes is produced by the well known Jahn–Teller effect [46].

Stepwise dissociation constants for all ligands (HL_n) and the stepwise stability constants of their complexes with Mn^{2+}, Co^{2+}, Ni^{2+} and Cu^{2+} have been calculated at 298, 308 and 318 K. The corresponding thermodynamic parameters (ΔG, ΔH and ΔS) were evaluated.

The dissociation constants (pK^H) for (HL_n), as well as the stability constants of their complexes with Mn^{2+}, Co^{2+}, Ni^{2+} and Cu^{2+} have been evaluated at 298, 308 and 318 K, and are given in Tables 7 and 9, respectively. The enthalpy (ΔH) for the dissociation and complexation process was calculated from the slope of the plot pK^H or log K vs. 1/T using the graphical representation of van't Hoff Eqs. (12) and (13):

$$\Delta G = -2.303\ RT\ \log K = \Delta H - T\Delta S \tag{12}$$

or

$$\log\ K = \left(\frac{-\Delta H}{2.303R}\right)\left(\frac{1}{T}\right) + \frac{\Delta S}{2.303R} \tag{13}$$

where R is the gas constant = 8.314 $J \cdot mol^{-1} \cdot K^{-1}$, K is the dissociation constant for the ligand stability and T is the temperature (K).

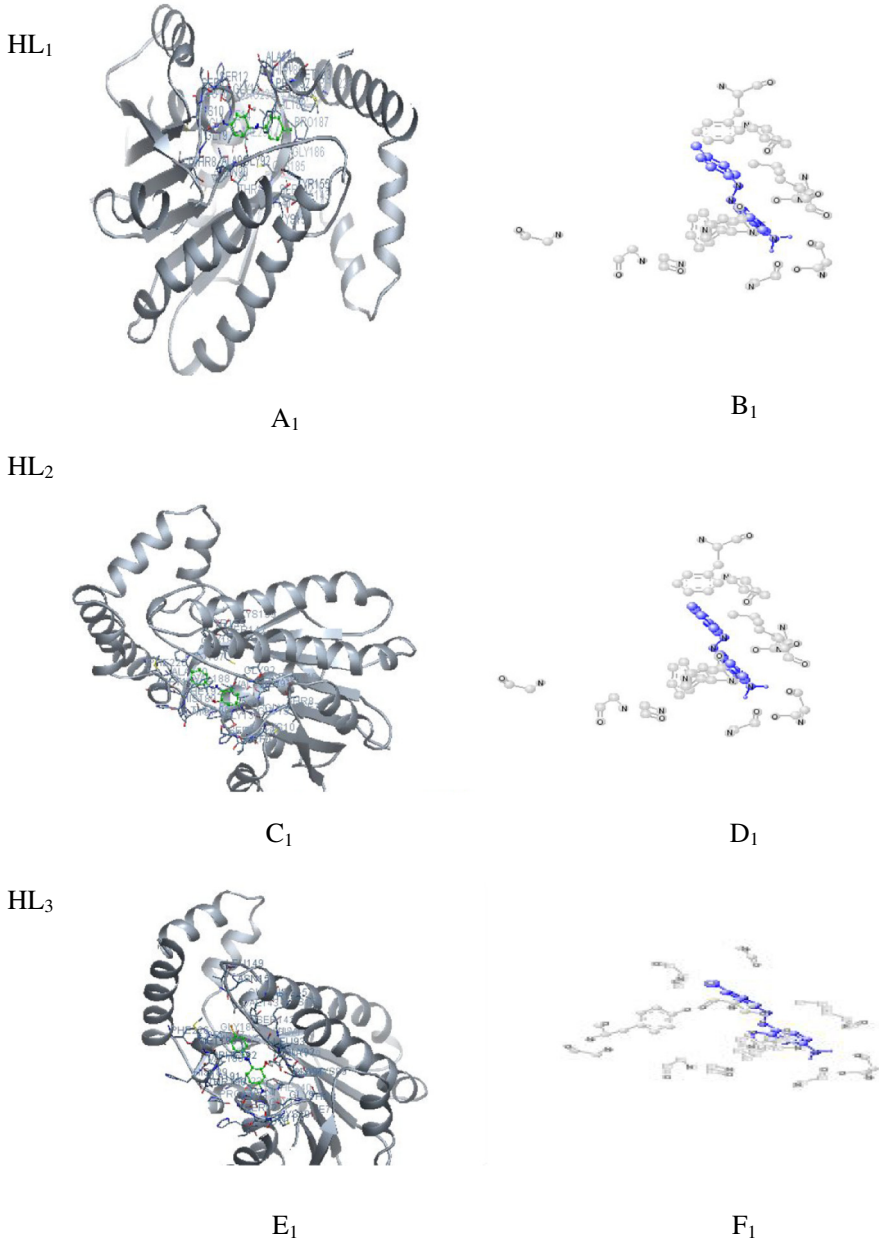

Fig. 5. The azo phenols (**HL_n**) (green in (A_1, C_1, E_1) and blue in (B_1, D_1, F_1)) in interaction with receptor breast cancer mutant 3hb5. (For interpretation of the references to color in this figure legend, the reader is referred to the web version of this article).

Table 5
Energy values obtained in docking calculations of azo phenols with receptor prostate cancer mutant 2q7k.

Ligand	Est. free energy of binding (kCal/mol)	Est. inhibition constant Ki (uM)	vdW + Hbond + desolv energy (kCal/mol)	Electrostatic energy (kCal/mol)	Total intermolec. energy (kCal/mol)	Interact surface
HL_1	−6.91	8.55	−8.04	−0.02	−8.06	477.708
HL_2	−2.76	9.46	−3.70	−0.15	−3.85	288.127
HL_3	−6.76	11.17	−7.69	−0.06	−7.75	483.220

Table 6
Energy values obtained in docking calculations of azo phenols with receptor breast cancer mutant 3hb5.

Ligand	Est. free energy of binding (kCal/mol)	Est. inhibition constant Ki (uM)	vdW + Hbond + desolv energy (kCal/mol)	Electrostatic energy (kCal/mol)	Total intermolec. energy (kCal/mol)	Interact surface
HL_1	−6.72	11.86	−7.35	−0.11	−7.46	687.618
HL_2	−6.78	10.76	−7.51	−0.11	−7.61	613.179
HL_3	−6.54	16.07	−7.87	−0.17	−8.04	696.115

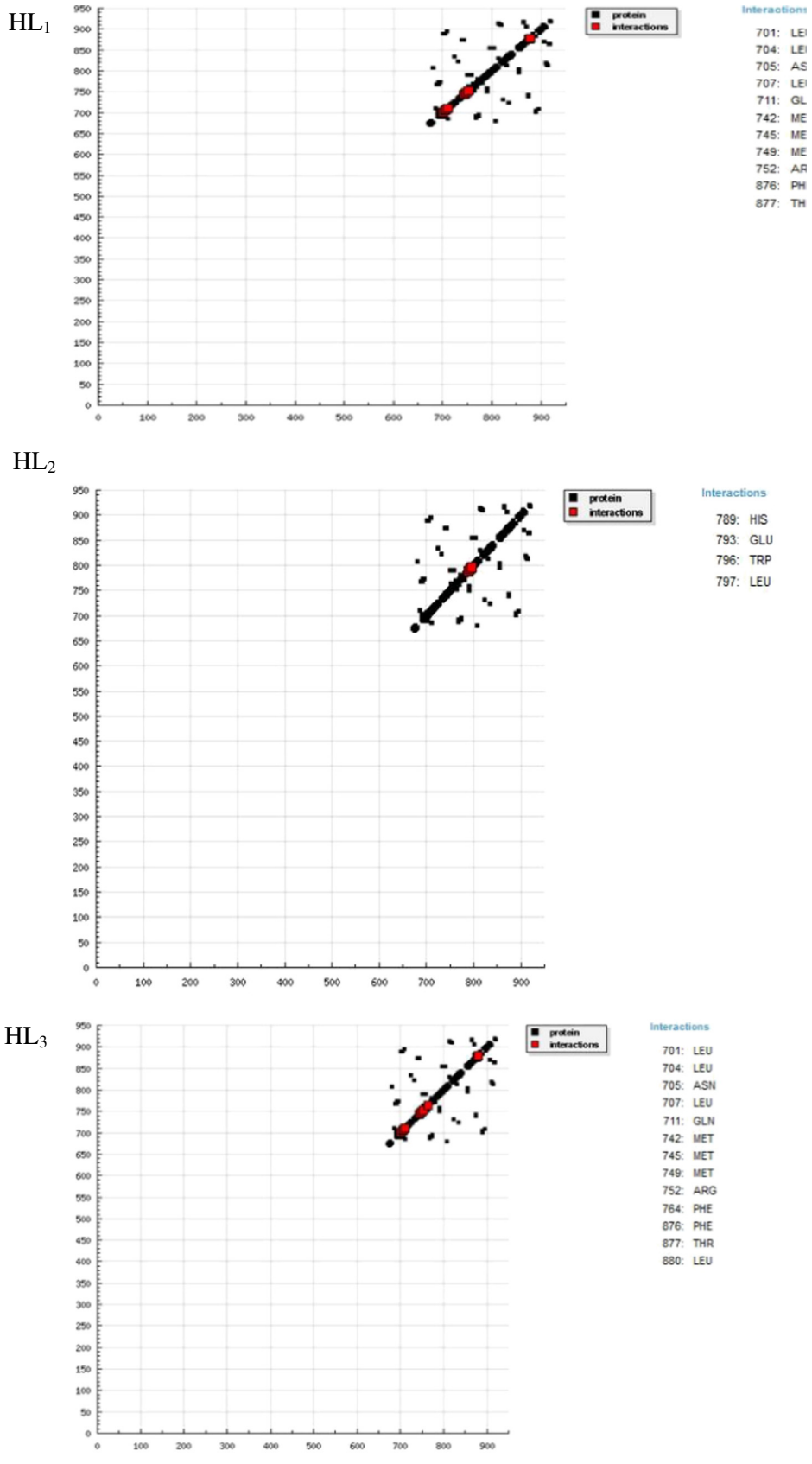

Fig. 6. HB plot of interaction between the azo phenols and receptor prostate cancer mutant 2q7k.

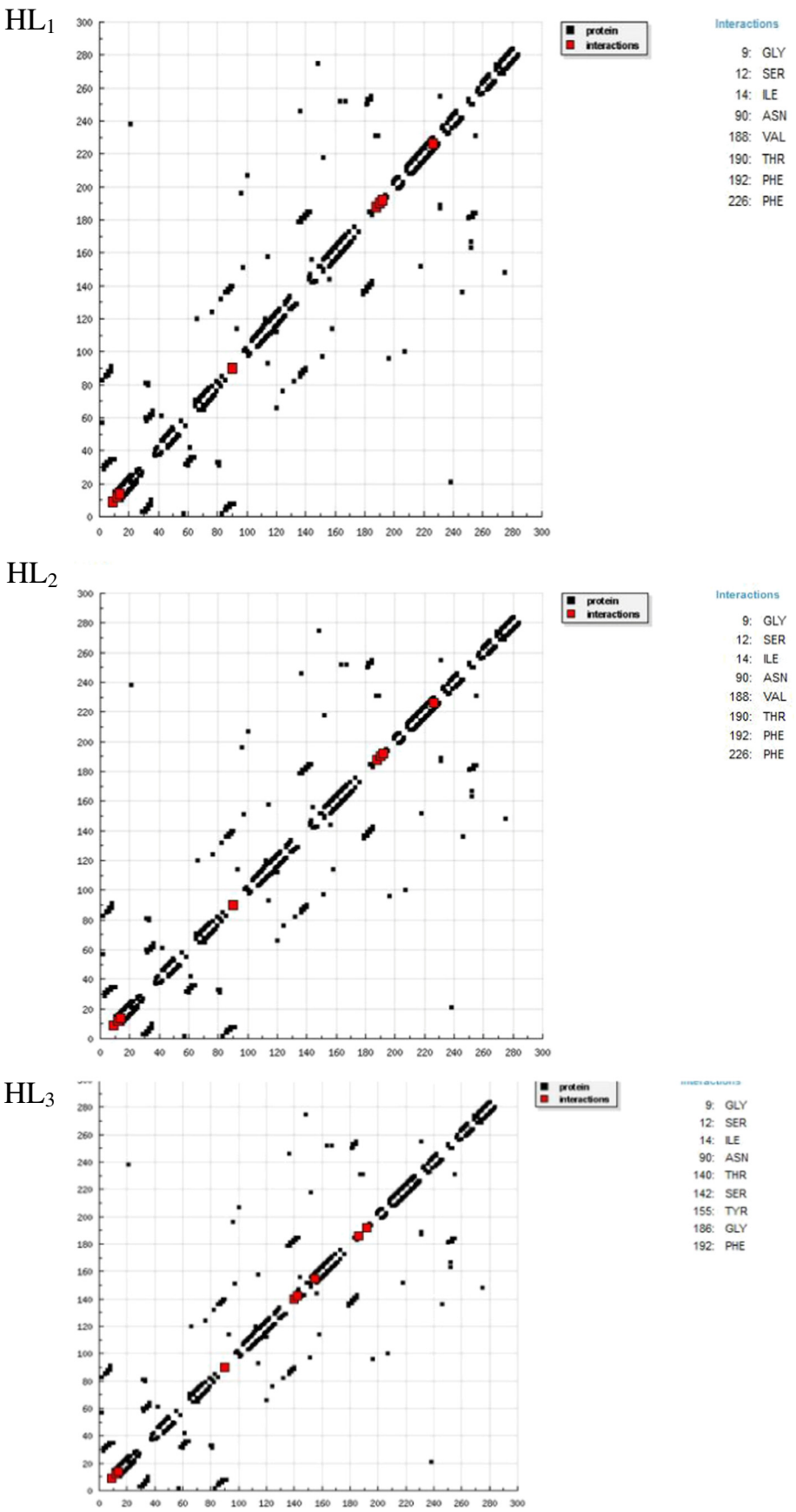

Fig. 7. HB plot of interaction between the azo phenols and receptor breast cancer mutant 3hb5.

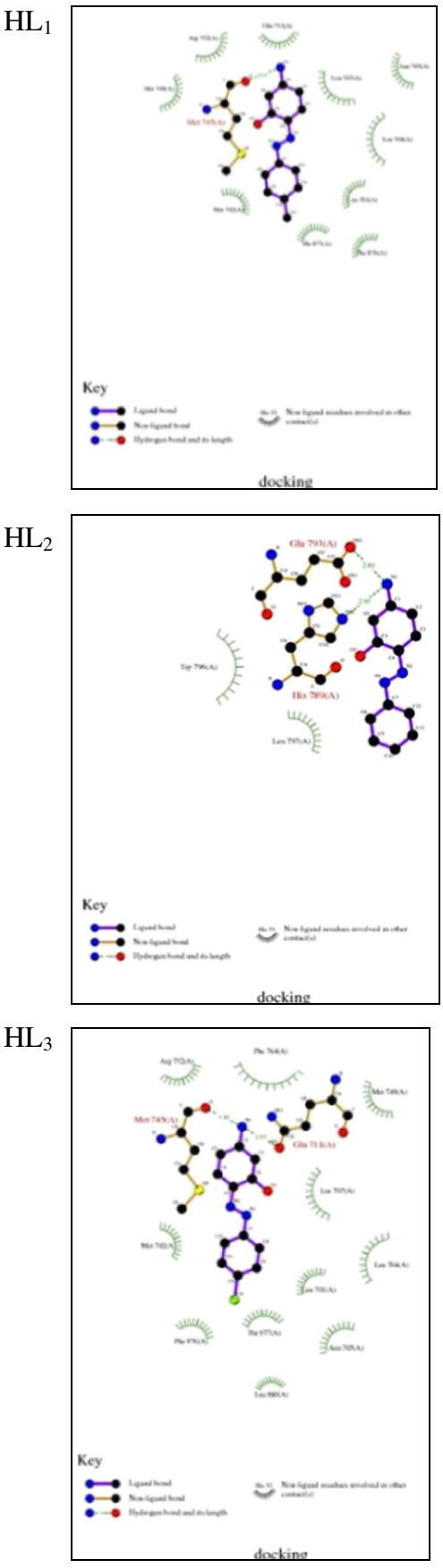

Fig. 8. 2D plot of interaction between the azo phenols and receptor prostate cancer mutant 2q7k.

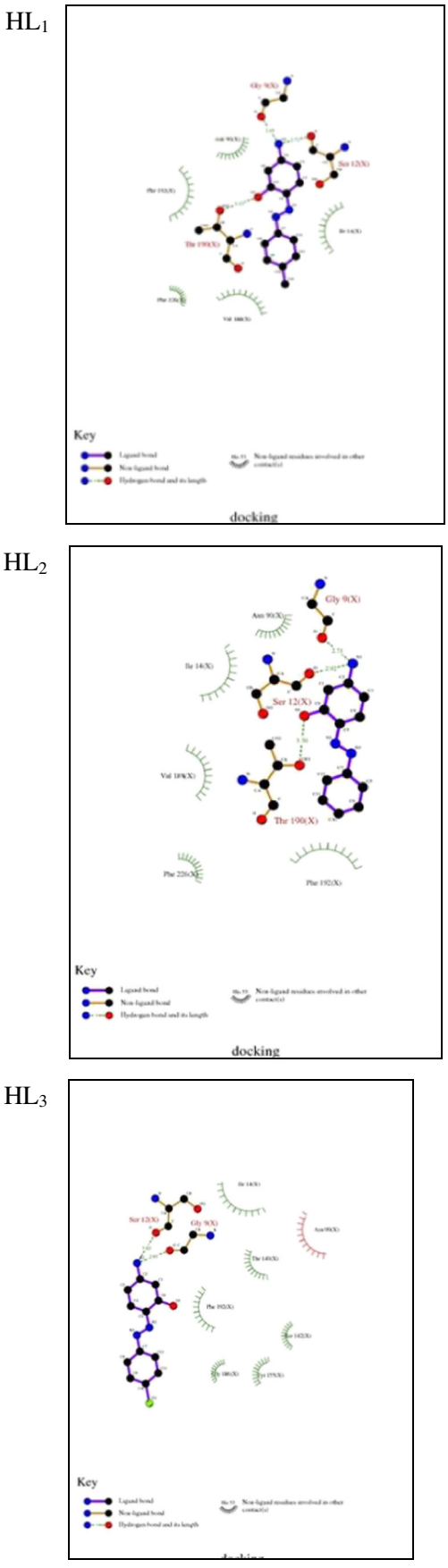

Fig. 9. 2D plot of interaction between the azo phenols and receptor breast cancer.

Table 7
Thermodynamic functions for the dissociation of (HL_n) in 40% (by volume) DMF–water mixture and 0.1 M KCl at different temperatures.

Compound	Temperature (K)	Dissociation constant pK^H	Gibbs energy kJ mol^{-1} ΔG_1	Enthalpy change kJ mol^{-1} ΔH_1	Entropy change J mol^{-1} K^{-1} $^{-}\Delta S_1$
HL_1	298	9.15	52.21		99.08
	308	9.02	53.19	22.68	99.06
	318	8.90	54.19		99.08
HL_2	298	9.02	51.47		108.76
	308	8.91	52.55	19.05	108.73
	318	8.81	53.64		108.77
HL_3	298	8.85	50.50		99.42
	308	8.73	51.48	20.87	99.40
	318	8.62	52.49		99.42

From the ΔG and ΔH values, one can deduce the entropy ΔS using the well known relationships (12) and (14):

$$\Delta S = (\Delta H - \Delta G)/T. \quad (14)$$

The thermodynamic parameters of the dissociation process of (HL_n) are recorded in Table 7. From these results the following can be made:

(i) The pK^H values decrease with increasing temperature, i.e. the acidity of ligand increases [15].
(ii) Positive values of ΔH indicate that dissociation is accompanied by absorption of heat and the process is endothermic.
(iii) Positive values of ΔG indicate that the dissociation process is not spontaneous [47].
(iv) Negative values of ΔS are due to increased order as result of the solvation processes.

All the thermodynamic parameters of stepwise stability constants for the complexes of ligand (HL_n) are recorded in Table 9. It is known that the divalent metal ions exist in solution as octahedral hydrated species [11,15] and the obtained values ΔH and ΔS can then be considered as sum of two contributions: (a) release of H_2O molecules and (b) metal–ligand bond formation. Examination of these values shows that:

(i) The stability constants (log K_1 and log K_2) for the azo aminophenol complexes increase with increasing temperature, i.e. its stability constants increase with increasing temperature.
(ii) The negative values of ΔG for the complexes' formation suggest a spontaneous nature of such process [13].
(iii) The positive values of ΔH mean that the complex formation processes are endothermic and favored at higher temperature.
(iv) The positive values of ΔS confirming that the complex formation processes are entropically favorable [11,13].

Table 8
Stepwise stability constants for complexes of (**HL_n**) in 40% (by volume) DMF–water mixtures and 0.1 M KCl at different temperatures.

Compound	298 K			308 K		318 K	
	M^{n+}	log K_1	log K_2	log K_1	log K_2	log K_1	log K_2
HL_1	Mn^{+2}	6.58	5.63	6.71	5.77	6.85	5.90
	Co^{2+}	6.68	5.70	6.80	5.83	6.93	5.97
	Ni^{2+}	6.76	5.78	6.88	5.90	6.99	6.04
	Cu^{2+}	6.89	5.88	6.99	6.02	7.12	6.15
HL_2	Mn^{2+}	6.45	5.51	6.60	5.65	6.72	5.78
	Co^{2+}	6.55	5.59	6.70	5.74	6.81	5.85
	Ni^{2+}	6.62	5.67	6.75	5.81	6.87	5.92
	Cu^{2+}	6.75	5.80	6.89	5.96	6.99	6.11
HL_3	Mn^{2+}	6.36	5.40	6.49	5.57	6.61	5.71
	Co^{2+}	6.45	5.49	6.58	5.64	6.68	5.78
	Ni^{2+}	6.53	5.57	6.68	5.69	6.79	5.86
	Cu^{2+}	6.64	5.70	6.77	5.81	6.90	5.99
HL_2	Mn^{2+}	6.45	5.51	6.60	5.65	6.72	5.78
	Co^{2+}	6.55	5.59	6.70	5.74	6.81	5.85
	Ni^{2+}	6.62	5.67	6.75	5.81	6.87	5.92
	Cu^{2+}	6.75	5.80	6.89	5.96	6.99	6.11
HL_3	Mn^{2+}	6.36	5.40	6.49	5.57	6.61	5.71
	Co^{2+}	6.45	5.49	6.58	5.64	6.68	5.78
	Ni^{2+}	6.53	5.57	6.68	5.69	6.79	5.86
	Cu^{2+}	6.64	5.70	6.77	5.81	6.90	5.99

Table 9
Thermodynamic functions for ML and ML_2 complexes of (**HL_n**) in 40% (by volume) DMF–water mixture and 0.1 M KCl.

Comp.	M^{n+}	T/K	Gibbs energy (kJ mol^{-1})		Enthalpy change (kJ mol^{-1})		Entropy change (J mol^{-1} K^{-1})	
			$-\Delta G_1$	$-\Delta G_2$	ΔH_1	ΔH_2	ΔS_1	ΔS_2
HL_1	Mn^{2+}	298	37.54	32.12	24.48	24.50	208.12	190.00
		308	39.57	34.03			207.95	190.01
		318	41.71	35.92			208.13	190.00
	Co^{2+}	298	38.12	32.52	22.66	24.48	203.95	191.28
		308	40.10	34.38			203.78	191.10
		318	42.20	36.35			203.96	191.28
	Ni^{2+}	298	38.57	32.98	20.87	23.56	199.46	189.73
		308	40.57	34.79			199.49	189.46
		318	42.56	36.78			199.46	189.74
	Cu^{2+}	298	39.31	33.55	20.83	24.50	201.82	194.79
		308	41.22	35.50			201.47	194.80
		318	43.35	37.45			201.83	194.79
HL_2	Mn^{2+}	298	36.80	31.44	24.52	24.50	205.77	187.70
		308	38.92	33.32			205.97	187.72
		318	40.92	35.19			205.76	187.70
	Co^{2+}	298	37.37	31.90	23.62	23.62	204.67	186.29
		308	39.51	33.85			204.97	186.59
		318	41.46	35.62			204.67	186.28
	Ni^{2+}	298	37.77	32.35	22.68	22.70	202.87	184.75
		308	39.81	34.26			202.89	184.95
		318	41.83	36.05			202.87	184.74
	Cu^{2+}	298	38.51	33.09	21.81	28.12	202.41	205.43
		308	40.63	35.15			202.72	205.43
		318	42.56	37.20			202.41	205.43
HL_3	Mn^{2+}	298	36.29	30.81	22.68	28.14	197.89	197.84
		308	38.27	32.85			197.91	198.03
		318	40.25	34.77			197.89	197.83
	Co^{2+}	298	36.80	31.33	20.89	26.31	193.59	193.41
		308	38.80	33.26			193.81	193.41
		318	40.67	35.19			193.59	193.41
	Ni^{2+}	298	37.26	31.78	23.62	26.25	204.29	194.74
		308	39.39	33.56			204.59	194.18
		318	41.34	35.68			204.28	194.75
	Cu^{2+}	298	37.89	32.52	23.58	26.23	206.26	197.16
		308	39.92	34.26			206.18	196.41
		318	42.01	36.47			206.27	197.18

An inspection of the results in Table 9 reveals that the pK^H values of (HL_2) and its substituted derivatives are influenced by the inductive or mesmeric effect of the substituents. HL_1 has a lower acidic character (higher pK^H values) than HL_3. This is quite reasonable because the presence of *p*-CH_3 group (i.e. an electron-donating effect) will enhance the electron density by their high positive inductive or mesomeric effect, whereby a stronger O–H bond is formed. The presence of *p*-Cl group (i.e. an electron-withdrawing effect) will lead to the opposite effect [15].

4. Conclusion

5-Amino-2-(phenyldiazenyl)phenol and its derivatives have been synthesized and characterized by different spectroscopic techniques. The molecular and electronic structures of the investigated compounds

(HL_n) were studied. The proton–ligand dissociation constant of (HL_n) and metal–ligand stability constants of their complexes with metal ions (Mn^{2+}, Co^{2+}, Ni^{2+} and Cu^{2+}) at different temperatures were determined. The stability constants of the formed complexes increase in the order Mn^{2+}, Co^{2+}, Ni^{2+} and Cu^{2+}. The dissociation process is non-spontaneous, endothermic and entropically unfavorable. The formation of the metal complexes has been found to be spontaneous, endothermic and entropically favorable. Molecular docking and binding energy calculations of azo phenols with the receptor of prostate cancer mutant indicated 2q7k and breast cancer 3hb5-oxidoreductase–Hormone provide that the presence of the azo phenol is an efficient inhibitor of prostate cancer mutant 2q7k-Hormone and breast cancer 3hb5-oxidoreductase.

References

[1] R. Bartnik, W. Strzyzewski, Pol. J. Appl. Chem. 36 (1992) 207–216.
[2] J.D. Talati, M.N. Desai, N.K. Shah, Anti-Corros. Meth. Mater. 52 (2005) 108–117.
[3] J.-S. Zhao, A. Singh, X.-D. Huang, O.P. Ward, Appl. Environ. Microbiol. 66 (2000) 2336–2342.
[4] R.J. Sorenson, J. Med. Chem. 19 (1976) 135–148.
[5] M.K. Alyaviya, Z.M. Tephyakova, Z.H. Neorgan, Khim. 10 (1995) 2504–2507.
[6] M. Gür, H. Kocaokutgen, M. Taş, Dyes Pigm. 72 (2007) 101–108.
[7] P. Gregory, High-technology Applications of Organic Colorants, Plenum Press, New-York and London, 1991.
[8] K. Yamaguchi, S. Kume, K. Namiki, M. Murata, N. Tamia, H. Nishihara, Inorg. Chem. 44 (2005) 9056–9067.
[9] E. Yuriev, M. Agostino, P.A. Ramsland, J. Mol. Recogn. 24 (2011) 149–164.
[10] T. Cheng, Q. Li, Z. Zhou, Y. Wang, S. Bryant, AAPS J. 14 (2012) 133–141.
[11] A.A. El-Bindary, A.Z. El-Sonbati, M.A. Diab, Sh.M. Morgan, J. Mol. Liq. 201 (2015) 36–42.
[12] A.Z. El-Sonbati, A.A. El-Bindary, R.M. Ahmed, J. Sol. Chem. 32 (2003) 617–623.
[13] A.Z. El-Sonbati, M.A. Diab, A.A. El-Bindary, Sh.M. Morgan, Inorg. Chim. Acta 404 (2013) 175–187.
[14] A.A. Al-Sarawy, A.A. El-Bindary, A.Z. El-Sonbati, M.M. Mokpel, Polish J. Chem. 80 (2006) 289–295.
[15] A.A. El-Bindary, A.Z. El-Sonbati, M.A. Diab, E.E. El-Katori, H.A. Seyam, Int. J. Adv. Res. 2 (2014) 493–502.
[16] A.Z. El-Sonbati, M.A. Diab, A.A. El-Bindary, A.M. Eldesoky, Sh.M. Morgan, Spectrochim. Acta A 135 (2015) 774–791.
[17] N.A. El-Ghamaz, A.Z. El-Sonbati, M.A. Diab, A.A. El-Bindary, G.G. Mohamed, Sh.M. Morgan, Spectrochim. Acta A 147 (2015) 200–211.
[18] R.G. Bates, M. Paabo, R.A. Robinson, J. Phys. Chem. 67 (1963) 1833–1838.
[19] H.M. Irving, M.G. Miles, L.D. Pettit, Anal. Chim. Acta 38 (1967) 475–488.
[20] G.H. Jeffery, J. Bassett, J. Mendham, R.C. Deney, Vogel's Textbook of Quantitative Chemical Analysis, 5th Edition Longman, London, 1989.
[21] M.M. Ghoneim, A.Z. El-Sonbati, A.A. El-Bindary, M.A. Diab, L.S. Serag, Spectrochim. Acta A 140 (2015) 111–131.
[22] N.A. El-Ghamaz, M.A. Diab, A.A. El-Bindary, A.Z. El-Sonbati, S.G. Nozha, Spectrochim. Acta A 143 (2015) 200–212.
[23] A.Z. El-Sonbati, M.A. Diab, A.A. El-Bindary, Sh.M. Morgan, Spectrochim. Acta A 127 (2014) 310–328.
[24] G.A. American Cancer Society, Cancer Facts & Figures, American Cancer Society, Atlanta, 2014.
[25] J.R. Benson, I. Jatoi, Future Oncol. 8 (2012) 697–702.
[26] A. Beteringhe, C. Racuciu, C. Balan, E. Stoican, L. Patron, Adv. Mater. Res. 787 (2013) 236–240.
[27] N.M. Hosny, M.A. Hussien, F.M. Radwan, N. Nawar, Spectrochim. Acta A 132 (2014) 121–129.
[28] Z. Bikadi, E. Hazai, J. Chem. Inf. 11 (2009) 1–15.
[29] T.A. Halgren, J. Comput. Chem. 17 (1998) 490–519.
[30] G.M. Morris, D.S. Goodsell, J. Comput. Chem. 19 (1998) 1639–1662.
[31] F.J. Solis, R.J.B. Wets, Mathemat. Operat. Res. 6 (1981) 19–30.
[32] E. Farkas, H. Csoka, J. Inorg. Biochem. 89 (2002) 219–226.
[33] M.M. Omar, G.G. Mohamed, Spectrochim. Acta A 61 (2005) 929–936.
[34] H. Irving, H.S. Rossotti, J. Chem. Soc. 74 (1953) 3397–3405.
[35] F.J.C. Rossotti, H.S. Rossotti, Acta Chem. Scand. 9 (1955) 1166–1176.
[36] M.T. Beck, I. Nagybal, Chemistry of Complex Equilibrium, Wiley, New York, 1990.
[37] A.A. El-Bindary, A.Z. El-Sonbati, E.H. El-Mosalamy, R.M. Ahmed, Chem. Pap. 57 (2003) 255–258.
[38] P. Sanyal, G.P. Sengupta, J. Ind. Chem. Soc. 67 (1990) 342–344.
[39] S. Sridhar, P. Kulanthaip, P. Thillaiarasu, V. Thanikachalam, G.J. Manikandan, World J. Chem. 4 (2009) 133–140.
[40] V.D. Athawale, V.J. Lele, Chem. Eng. Data 41 (1996) 1015–1019.
[41] V.D. Athawale, S.S. Nerkar, Monatsh. Chem. 131 (2000) 267–276.
[42] G.A. Ibañez, G.M. Escandar, Polyhedron 17 (1998) 4433–4441.
[43] W.U. Malik, G.D. Tuli, R.D. Madan, Selected Topics in Inorganic Chemistry, 3rd Edition Chand S. & Company LTD, New Delhi, 1984.
[44] G.G. Mohamed, M.M. Omar, A. Ibrahim, Eur. J. Med. Chem. 44 (2009) 4801–4812.
[45] F.R. Harlly, R.M. Burgess, R.M. Alcock, Solution Equilibria, Ellis Harwood, Chichester, 1980. 257.
[46] L.E. Orgel, An Introduction to Transition Metal Chemistry Ligand Field Theory, 1966. 55 (Methuen, London).
[47] A. Bebot-Bringaud, C. Dange, N. Fauconnier, C. Gerard, J. Inorg. Biochem. 75 (1999) 71–78.